MODEL-BASED CONTROL OF SUBSURFACE FLOW

Jan-Dirk Jansen

*Delft University of Technology, Department of Geotechnology, The Netherlands, and
Shell International Exploration and Production, Exploratory Research, The Netherlands*

Abstract: An emerging method to increase the recovery from oil reservoirs is the application of measurement and control techniques to better control subsurface flow over the life of the reservoir. In particular the use of sensors and remotely controllable valves in wells and at surface, in combination with large-scale subsurface flow models is promising. Various elements from process control may play a role in such 'closed-loop' reservoir management, in particular optimization, parameter estimation and model reduction techniques. *Copyright © 2007 IFAC*

Keywords: petroleum, production, model-based, control, optimization, system, identification, data assimilation, parameter estimation, adjoint, robust, model reduction.

1. INTRODUCTION

An increasing quality of life of the world's increasing population will result in an increasing energy demand for the decades to come. Although the contribution of sustainable energy sources (hydro, wind, solar and biomass) is slowly going up, fossil fuels (oil, gas and coal) will remain to play a very important role until at least the end of this century; see e.g. Smil (2003). An increasing problem, in particular for oil, is that the 'easily' producible reservoirs have nearly all been found (to our current knowledge), and to a large extent been produced. Most oil fields consist of relatively thin slabs of porous rock buried at depths of hundreds to thousands of meters. After the drilling of wells the oil usually flows to the surface naturally, but after some years this primary recovery phase ends, and it will be necessary to inject water or gas into the reservoir to maintain the reservoir pressure and to displace the oil from the injection wells towards the production wells. However, even when using such secondary recovery techniques, most of the oil remains trapped in the pores of the rock, and often the oil recovery factor stays somewhere between 10 and 50%. Increasing the recovery factor of existing oil fields is therefore a good alternative to finding new ones. Sometimes this is possible during a tertiary recovery phase through the use of 'enhanced' oil recovery techniques such as the injection of surfactants, polymers or steam. These techniques are relatively expensive, and, depending on the type of oil and the subsurface conditions, only economically

feasible at oil prices even above the current high level. An alternative, emerging, method to increase the recovery factor is the application of measurement and control techniques to improve the control of subsurface flow. In particular the use of sensors and remotely controllable valves in wells and at surface, in combination with large-scale subsurface flow models is an increasing area of research, which is known in the oil industry under various names, such as 'smart fields', 'intelligent fields', 'real-time reservoir management', or 'closed-loop reservoir management'. Many of the 'smart' applications of measurement and control in wells were initially focused on increasing the instantaneous production rate, i.e. on short term 'production management', through the use of 'reactive' control strategies. Here we will consider long term 'reservoir management' with the aim to maximize recovery, or some economic objective function, over the life of the reservoir, see Fig. 1. This typically requires a more 'pro-active' approach using system models to predict future performance. Sources of inspiration for our research are at one hand model-based control concepts as used in the process industry, which offer a wide variety of solutions to cope with uncertainties, nonlinearities and multi-scale optimization. At the other hand we draw inspiration from disciplines like meteorology and oceanography where advanced data assimilation techniques have been developed to condition large scale flow models (with more than 10^6 state variables) to measured data while honoring measurement and model errors.
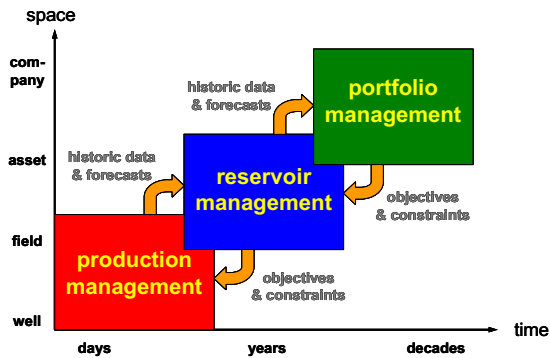
Fig. 1. Domains in time and space covering the main elements of the oil recovery process.

2. RESERVOIR MANAGEMENT

Fig. 2 depicts reservoir management as a model-based controlled process (Jansen et al. (2005)). The system, at the top of the figure, comprises of one or more reservoirs, wells, and facilities for the separation and treatment of oil, gas and water. Generally, the system boundaries can be specified accurately for the wells and the surface facilities, but are much more uncertain for the reservoir of which the geometry is usually deduced from seismics with a limited resolution. Also the parameters of the system are known to varying degrees: the fluid properties can usually be determined quite well, but the reservoir properties are only really known at the wells. The subsurface is very heterogeneous, and the parameters relevant to flow are correlated at different length scales, but often over distances smaller than the well spacing. As a consequence, the uncertainties in the model parameters of the subsurface part of the system are very large, and during the design phase of an oil field development it is therefore customary to construct multiple subsurface models to simulate the flow of fluids for different geological 'realizations'. The typical number of state variables in these system models is in the order of 10^4 to 10^6, with similar numbers for the model parameters. Numerical simulation of reservoir flow is performed in discrete time steps of weeks to months and a single forward run, i.e. simulation of some decades of oil production, typically involves hours to tens of hours computing time. Based on these large-scale system models it is possible to optimize the oil recovery process design (known as the field development plan). This concerns, for example, determining the number and position of wells, or the optimal water injection and oil production flow rates over the life of the reservoir. During the past decades the possibilities to control subsurface flow have increased considerably. This concerns complex well configurations, e.g. 'meandering' horizontal wells, or multi-lateral wells with multiple branches, and the installation of control valves in 'smart' wells or at surface. Model-based optimization is therefore a rapidly growing activity within the reservoir simulation community. This optimization process is indicated in blue in Fig. 2. During the oil production process, more or less regular measurements are performed at the top of the wells and in the facilities, which give an indication of the pressures and phase rates (i.e. oil, gas and water flow rates) in the surface

part of the production system. Traditionally these measurements are performed monthly or quarterly and with a limited accuracy. During the past years, however, an increasing amount of sensors is being installed that give near-continuous information about the system pressures and phase rates, not only at surface but more and more also downhole. In addition, other measurement techniques have emerged that give an impression of the changes in reservoir pressure and fluid saturations in between the wells. This concerns in particular 'time-lapse' seismic measurements, which allow for monitoring the displacement of oil-water or oil-gas fronts between injection and production wells at regular (say quarterly to yearly) intervals. By combining the measured response of sensors and the simulated response of the system models it is possible to judge to what extent the models represent reality. With the aid of systematic algorithms for data assimilation it is then, to some extent, possible to adjust the system parameters such that the simulated response better matches with the measured data, and, hopefully, such that the models give better predictions of the future system response. The development of 'automatic history matching' techniques is therefore another area of current activity in reservoir simulation research. The data assimilation process is indicated in red in Fig. 2.
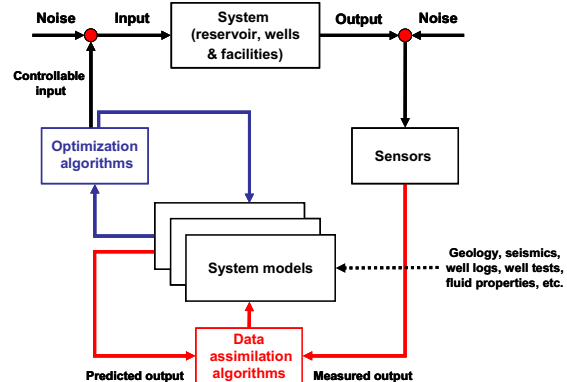

Fig. 2. Reservoir management depicted as a closed-loop model-based controlled process.

3. SYSTEM EQUATIONS

3.1. Notation

All our work is based on the use of numerical reservoir models. We express the model equations in state space notation. Vectors are indicated with Roman or Greek lower case letters, either in bold face or in index notation. Matrices are indicated with Roman or Greek capitals. The superscript T is used to indicate the transpose, and dots above variables to indicate differentiation with respect to time t.

3.2. Reservoir models

We consider models for multiphase flow through porous media. Starting from the governing partial differential equations and boundary conditions, and applying a semi-discretization in space (using e.g. finite differences, finite elements or finite volumes) we obtain a set of ordinary differential equations that

can be expressed as (see Appendix A for a derivation)

$$\dot{\mathbf{x}} = \mathbf{f}(\mathbf{x}, \mathbf{u}, \boldsymbol{\theta}) \;, \tag{1}$$

or, even more general, as

$$\mathbf{g}(\dot{\mathbf{x}}, \mathbf{x}, \mathbf{u}, \boldsymbol{\theta}) = \mathbf{0} \;, \tag{2}$$

where $\mathbf{f}$ and $\mathbf{g}$ are nonlinear vector-valued functions, $\mathbf{x}$ is the state vector, $\mathbf{u}$ the input vector (control vector), and $\boldsymbol{\theta}$ a vector of model parameters. In a conventional iso-thermal reservoir simulation model, $\mathbf{x}$ typically contains pressures and phase saturations or component accumulations, $\mathbf{u}$ contains the well flow rates, well pressures, or valve settings in those grid blocks that are penetrated by wells, and $\boldsymbol{\theta}$ contains parameters like porosities, permeabilities and other reservoir and fluid properties. Using some form of time discretization, the continuous-time equation (2) can be rewritten in discrete-time form as

$$\mathbf{g}(\mathbf{x}_{k+1}, \mathbf{x}_k, \mathbf{u}_k, \boldsymbol{\theta}) = \mathbf{0} \;, \tag{3}$$

where the subscript k indicates discrete time. To complete the model we need to specify initial conditions, which, in the discrete case, can be represented as

$$\mathbf{x}_0 = \hat{\mathbf{x}} \;. \tag{4}$$

Output variables y, combined in an output vector $\mathbf{y}$, are a function of the state variables $\mathbf{x}$, according to

$$\mathbf{y}_k = \mathbf{h}(\mathbf{x}_k) \;, \tag{5}$$

where $\mathbf{h}$ is a vector-valued function. Typical outputs are wellbore pressures and phase flow rates, either measured at surface or downhole. Note: Although in this paper we use a notation that is quite obvious to control engineers, the notation used in the reservoir engineering literature will often be less familiar.

3.3. Nature of the equations

As discussed in some more detail in Appendix A, the governing equations for multi-phase flow through porous media are a set of mildly nonlinear parabolic (diffusion) equations, describing the rate of change of pressures, coupled to a set of strongly nonlinear parabolic-hyperbolic (diffusion-convection) equations, describing the rate of change of phase saturations or component concentrations. The very low flow rates imply that inertia effects may usually be neglected. Moreover, the flow is strongly dissipative, such that the response to disturbances is typically over-critically damped and instability of the flow in time is not an issue. (Numerical instabilities during simulation of the discretized equations may of course still occur, notably when the solution methods used are not fully implicit.) The time constants of the pressure equation are typically in the order of hours to months, whereas the diffusive parts of the saturation equations may have time constants up to thousands of years. Also the convective terms (i.e. the fluid velocities) are usually so small that the propagation speeds of oil-water or oil-gas fronts are typically much lower than those of the pressure waves. Under some mild assumptions the pressure equations may therefore often be approximated as linear with slowly time-varying coefficients. The

saturation equations are inherently nonlinear, and in the limit of zero diffusion may exhibit typical properties of hyperbolic equations such as shocks and rarefaction waves. The coefficients of the equations are generally very poorly known, and moreover often vary spatially up to four orders of magnitude.

4. OPTIMIZATION

4.1. Optimization methods

For a given configuration of wells, and in particular for a flooding scenario involving multiple injectors and producers, we can use the well rates or pressures to optimize the flooding process over the life of the reservoir. First we will address optimization without updating of the reservoir model, i.e. the blue loop in Fig. 2. As in any optimization problem, we need an objective function and constraints. For example, the objective could be to maximize recovery or the net present value of the water flooding process. Generally, the objective function can be expressed as:

$$J = \sum_{k=1}^{K} J_k(\mathbf{y}_k, \mathbf{u}_k) \;, \tag{6}$$

where K is the total number of time steps, and where J_k represents the contribution to J in each time step (e.g. the sum of oil revenues and water injection and production costs during that time interval, where the costs have a negative value). Constraints can be expressed in terms of the state variables or the input variables and may be equality or inequality constraints, which we represent in a general form as

$$\mathbf{c}(\mathbf{x}_k, \mathbf{u}_k) \leq \mathbf{0} \;. \tag{7}$$

The control problem can now be formulated as finding the control vector $\mathbf{u}_k$ that maximizes J over the time interval $k = 1, \ldots, K$, subject to system equations (3), initial conditions (4), output equations (5) and constraints (7). Many numerical techniques are available to solve this optimization problem. In our work we have been using a gradient-based optimization technique where the derivative information is obtained through the use of an adjoint equation; see Brouwer and Jansen (2004), Van Essen et al. (2006) and Zandvliet et al. (2007). Much earlier, adjoint-based techniques were introduced in reservoir engineering for the optimization of tertiary recovery processes such as polymer or CO_2 flooding; see Ramirez (1987). The first paper on gradient-based control of water flooding is Asheim (1988), followed by, among others, Virnovsky (1991), Zakirov et al. (1996) and Sudaryanto and Yortsos (2000). However, industry uptake of these methods was almost absent until quite recent, when the advent of 'smart well' and 'smart fields' technology caused a revival of interest. Gradient-based optimization methods make use of the derivatives $\partial J / \partial u_{ik}$, to guide the iteration process. Here, u_{ik} is a single element i of vector $\mathbf{u}_k$ at time k. Gradient-based methods generally require much less function evaluations than gradient-free methods, but at the price of having to compute the derivatives at every iteration step. Alternative methods to perform field-

life optimization, and in particular those addressing well placement optimization, use 'non-classical' methods such as genetic algorithms; see e.g. Yeten et al. (2003) and Güyagüler and Horne (2004). Moreover, applications to optimize more complex reservoir flow processes, such as alternating-water-gas (WAG) injection, are beginning to receive more attention, sometimes in combination with reduced-physics models such as streamline models or response surfaces generated with experimental design (Esmaiel et al. (2005)).

4.2. Optimal control

A very efficient way to obtain gradients of the objective function J with respect to the inputs $\mathbf{u}_k$ is given by 'optimal control theory' which makes use of an adjoint formulation; see e.g. Stengel (1994). Once the gradients have been obtained, a wide variety of gradient-based techniques is available to iterate to a (locally) optimal solution; see e.g. Gill et al. (1981). Appendix B gives a brief overview of adjoint-based optimization. Implementation of the adjoint formulation in a numerical reservoir simulator is conceptually simple if the simulator is fully implicit, because in that case the Jacobian matrix $\partial \mathbf{g}_k / \partial \mathbf{x}_k$, which is required in the adjoint formulation, is already available; see Sarma et al (2005). In practice the programming effort is still considerable because of the complexity of modern reservoir simulation programs, which may contain up to millions of lines of code. Another, more theoretical, problem is the systematic incorporation of the constraints $\mathbf{c}$ as specified in equation (7). Some possible solutions are given in Sarma et al. (2006a), Montleau et al. (2006), and Kraaijevanger et al. (2007). One of the disadvantages of gradient-based techniques is their tendency to arrive at a local optimum rather than a global one. This is particularly the case if we have a large number of controls (wells) and a large number of points in time at which we may change the control setting, resulting in a very large number of possible control trajectories. Several regularization techniques can be applied to 'smooth' the control trajectories and to limit the freedom in choosing control settings. Although this may result, theoretically, in a sub-optimal global optimum, it will hopefully result in less local optima, and in an increased speed of the iterative optimization process; see e.g. Stengel (1994). An adaptive multi-scale regularization technique for water flooding optimization was implemented by Lien et al. (2006). Recently we also started to investigate the use of adjoint-based techniques to optimize well locations, and the first results are promising; see Handels et al. (2007).

4.3. 'Smart well' optimization

The implementation of a dynamic water flooding optimization strategy, as e.g. obtained with the aid of optimal control theory, requires the availability of adjustable valves. Mostly, wells are controlled at the 'well head', i.e. at the point where the well reaches the surface. A recent development are so-called 'smart wells', equipped with down hole 'inflow control valves' which allow for the inflow control of individual well segments in one or more reservoirs penetrated by the well; see Fig. 3. Initially, the use of smart well technology was strongly focused on short-term production optimization; see e.g. Naus et al. (2006). However, as shown in Brouwer and Jansen (2004) and in several publications thereafter, there may be considerable scope to achieve increased ultimate recovery using optimal control over the entire life of the reservoir. In the operational practice of controlling wells it is often more convenient to simply switch off a well rather than to try to keep its production at a predefined rate or pressure. Moreover, on/off valves are also cheaper than continuously variable valves, especially downhole valves which may cost tens of thousands of dollars each. Fortunately, some water flooding control problems appear to have an optimal solution that is close to or sometimes equal to 'bang-bang', i.e. it is an optimal strategy to just open or close valves rather than to gradually adjust them; see Zandvliet et al. (2007). Maybe somewhat surprisingly, hardly any attention has been paid to the use of (nonlinear) model-predictive control (NMPC) techniques, or even to just performing optimal control with a receding horizon, with the exception of the work of Saputelli et al. (2006). Indeed there appear to be ample opportunities to investigate the use of NMPC, and possibly other optimization techniques from the process control community, for reservoir flooding optimization.

4.4. Robust control

One of the major challenges in reservoir engineering is taking decisions in the presence of very large uncertainties about the subsurface structure and the parameters that influence fluid flow. Reservoirs are inhomogeneous and usually consist of fossilized deltaic or fluvial deposits (sand, clay, carbonates) with a distinct layering and sometimes a complicated network of fractures. They have often been tilted, faulted or otherwise deformed. Seismic information has a resolution that is generally too coarse to determine the individual geological layers in detail. Borehole measurements, using a whole range of physical measurement principles, give a much more detailed picture of the subsurface, but are scarce and only truly representative for a small area around the wells. As was already indicated in Fig. 2, one of the ways to cope with this uncertainty during the field development phase of a reservoir is to use multiple subsurface models, also known as geological realizations. In that case we would also like to perform the optimization over the ensemble of realizations, but because we can only use one optimization strategy for the real field, we need to average the results in some sense.
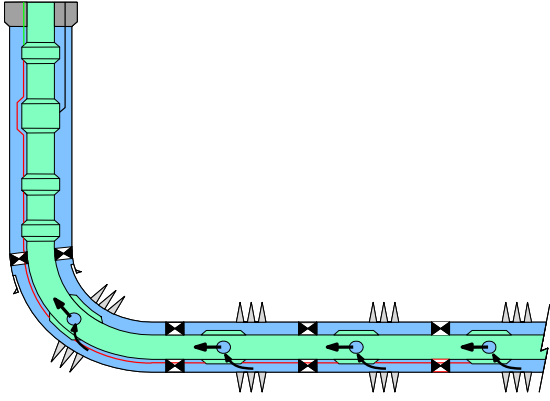
Fig. 3. Schematic representation of a 'smart' horizontal well, equipped with an inner tube (green) and an outer tube, and valves to control the inflow from the reservoir into the individual segments of the well. The grey triangles represent openings that connect the reservoir to the (blue) annular space between the inner and outer tube. The small blue circles represent the remotely controllable inflow control valves.

Recently we developed a robust control strategy through computing the expected value of the objective function J as

$$E_{\boldsymbol{\theta}}\left(J\right) \approx \frac{1}{N_R}\sum_{i=1}^{N_R}J\left(\mathbf{y},\mathbf{u},\boldsymbol{\theta}^i\right) \qquad (8)$$

where $\boldsymbol{\theta}^i$ are the parameter vectors of realizations $i =1, …, N_R$; see van Essen et al. (2006). As an example, consider Fig. 4 which displays two equiprobable realizations, out of an ensemble of 100, of a reservoir that has a fluvial structure with high-permeability sandstone channels (green) in a background of low permeability claystone (blue). Fig. 5 displays the results, expressed as a cumulative distribution function of the financial performance measure (objective function) J, for three optimization methods, as applied to the hundred realizations. The blue curve corresponds to an often used reactive water flooding strategy, where the production wells are shut-in once the water/oil ratio exceeds a preset maximum. The green curve corresponds to a nominal optimization strategy based on a single 'best' realization. The red curve corresponds to the robust optimization strategy based on hundred realizations, and the purple curve to the same robust strategy but applied to a different set of 100 realizations drawn from the same population of reservoir models. The curves clearly show the value of optimization over reactive control, and the additional benefit of a robust optimization strategy: not only is the mean (at the horizontal dotted line) highest for the robust results, also the standard deviation is lowest (steepest curves).

5. DATA ASSIMILATION

5.1. Formulation as optimization problem

Data assimilation, or automatic history matching, is the adaptation of the states and parameters of a system model to measured data, as indicated in red in Fig. 2. In our case this implies updating states $\mathbf{x}$ and parameters $\boldsymbol{\theta}$ using measured output data $\mathbf{y}_m$.
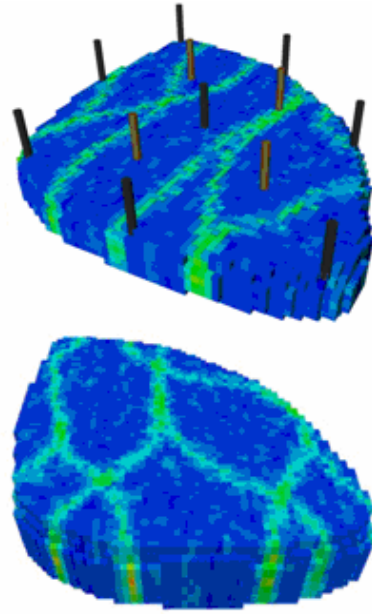

Fig. 4. Two equiprobable realizations of a channelized reservoir. The top figure shows the 4 production wells (brown) surrounded by 8 water injection wells (black). (Van Essen et al. (2006)).
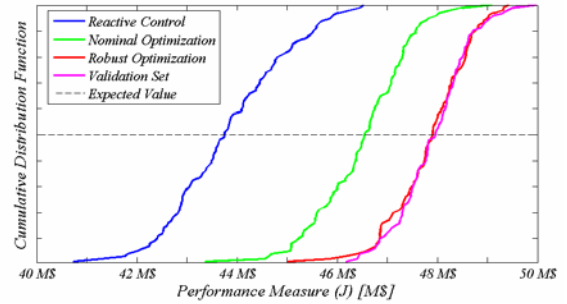

Fig. 5. Cumulative distribution functions for three different control strategies. (Van Essen et al. (2006)).

Often the history matching problem is formulated as an optimization problem for the parameters only, with an objective function defined in terms of the mismatch between measured and simulated output data:

$$J = \sum_{i=1}^{\kappa}\left[\left(\mathbf{y}_m^i - \mathbf{y}^i\right)^T \mathbf{R}_y^{-1}\left(\mathbf{y}_m^i - \mathbf{y}^i\right)\right], \qquad (9)$$

where $\mathbf{R}_y$ is a weight matrix which is often chosen as the spatial covariance matrix of the measurement errors, and where the counter $i = 1, …, \kappa$ indicates the measurements at different points in time. The optimization problem is then usually solved with the aid of an adjoint-based method; see e.g. Chavent et al (1975) and Li et al. (2003). Often the objective function is expanded to include a term that penalizes large deviations between the updated parameter values $\boldsymbol{\theta}_u$ and the prior values $\boldsymbol{\theta}$:

$$\begin{aligned} J = \sum_{i=1}^{\kappa}\Big[&\left(\mathbf{y}_m^i - \mathbf{y}^i\right)^T \mathbf{R}_y^{-1}\left(\mathbf{y}_m^i - \mathbf{y}^i\right) \\ &+ \left(\boldsymbol{\theta}_u^i - \boldsymbol{\theta}^i\right)^T \mathbf{R}_\theta^{-1}\left(\boldsymbol{\theta}_u^i - \boldsymbol{\theta}^i\right)\Big]. \end{aligned} \qquad (10)$$

The weight matrix $\mathbf{R}_\theta$ can be interpreted as a parameter error covariance matrix. If the states are also updated, the uncertainty is taken into account with an additional covariance matrix $\mathbf{R}_x$. Joint updating of states and parameters can be done using the 'representer method' which was first introduced in ocean engineering; see Bennett (2002). For early applications to reservoir engineering, see Rommelse et al. (2006), and Przybysz-Jarnut et al. (2007). An alternative way to cope with model uncertainties is through the use of the ensemble Kalman filtering method, which we will briefly discuss below. Specialized model updating methods have been developed in the reservoir engineering community using, e.g., streamline simulation to rapidly derive sensitivities of saturation changes along streamlines (Vasco et al. (1999)). Other specialized methods perform history matching under geostatistical constraints, such as the probability perturbation method (Caers (2003)), or emphasise the quantification of uncertainty; see e.g. Erbaş and Christie (2007).

5.2. Ensemble Kalman filtering

As is well known in the process control community, the minimization problem to estimate states as described above may also be formulated as a sequential estimation procedure, i.e. such that the data are assimilated whenever they become available. It can be shown that for linear systems, and assuming Gaussian measurement and process noise, this sequential 'Kalman filter' approach results in exactly the same answers as the representer method (Bennett (2002)). For nonlinear problems, the ordinary Kalman filter breaks down because the nonlinearity results in non-Gaussian noise when propagated through the system. In the ensemble Kalman filter (EnKF) the analytical error propagation is replaced by a Monte Carlo approach: the model error covariance is computed from an ensemble of model realizations which are all propagated in time. This ensemble method has proved very successful in oceanographic applications where very large models, containing millions of state variables, are frequently updated using a variety of data sources; see Evensen (2006). During the forecast step a simulation is run for each of the model realizations up to the time where new measurements become available. With these measurements, all realizations in the model are updated by combining the new real measurements with forecasts from the ensemble. Recently a large number of publications have appeared that apply the EnKF to reservoir engineering problems; see e.g. Nævdal et al. (2005), Reynolds (2006) and Evensen (2006). These implementations of the EnKF also treat parameters as unknowns, which leads to the use of an extended state vector $\widehat{\mathbf{x}} = [\mathbf{x}^T \, \boldsymbol{\theta}^T]^T$.

5.3. Parameterization

In our parameter and state estimation problems we are dealing with a very large number of 'inputs' (parameters and states) that need to be adjusted to obtain a best match between modeled and real data.

A typical reservoir model may contain millions of unknown parameters, such as grid block permeabilities and porosities, fault transmissibilities and initial conditions. Fortunately most of these parameters display spatial correlations that can be used to reduce the dimension of the parameter space, and various techniques to regularize the parameter estimation problem have been proposed using, e.g., zonation, wavelets, Karhunen-Loève decomposition or discrete cosine transforms; see Jafarpour and McLaughlin (2007) for a recent overview. It has been shown that it is also possible to make use of spatial correlations in the states (pressures, saturations) to reduce the order of reservoir models using system theoretical techniques, but application of these possibilities either in optimization or in data assimilation has hardly yet been pursued. For some early attempts, see Heijn et al. (2004), Van Doren et al. (2006), Markovinović and Jansen (2006), and Gildin et al (2006). In general the amount of information that can be obtained from well data is rather limited, especially because the pressure propagation through a reservoir is a diffusive process. Sometimes it is possible to obtain areal information through the repetition of seismics in time, which may give an indication of those reservoir areas where pressures or saturations have changed. However, the data obtained from production measurements and time-lapse seismics are never sufficient to fully characterize the states and parameters in a reservoir, and history matching is therefore an inherently ill-posed problem. Especially if reservoir models are used for field re-development planning, involving e.g. the drilling of new wells, geological models are essential to constrain the solution space of the data assimilation problem. Surprisingly, a formal analysis of the observability and identifyability of reservoir flow and the identifyability of the model parameters, has, to our knowledge, not yet been reported and there appears to be ample scope to clarify these system-theoretical aspects of subsurface flow.

6. CLOSED-LOOP RESERVOIR MANAGEMENT

Finally, we consider an example of full closed-loop reservoir management, as indicated in Fig. 1, by combining optimization (the 'blue loop') with data assimilation (the 'red loop'). The results are taken from Overbeek et al. (2004), and are comparable to other early results reported in Brouwer et al (2004), Nævdal et al. (2006) and Sarma et al. (2006b). Fig. 6 depicts a reservoir modeled with 12100 grid blocks which was used as 'truth' to generate synthetic 'measured' data. The 10 crosses at the left represent a row of vertical water injection wells, and the 10 circles at the right a row of producers. Just as in the previous example, the reservoir contains high-permeability sandy channels (in red) amidst a low-permeability clayish background (blue). We assumed that noisy measurements of pressure and total flow rate (oil plus water) were available in all wells. We used optimal control theory with a steepest descent method for the flooding optimization and the EnKF method for updating the unknown grid block permeabilities in the ensemble of reservoir models.
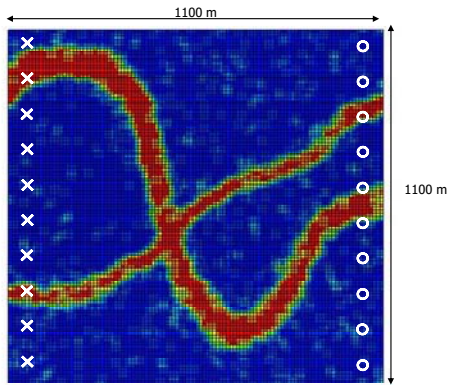
Fig. 6. Top view of the 'true' reservoir used to generate synthetic data. (After Overbeek et al. (2004))

The optimization objective was oil revenue minus water production costs. The top row in Fig. 7 depicts the snapshots in time of a conventional flooding strategy. As expected, the injected water rapidly flows through the highly permeable channels, which results in early water production in some of the producers. After one pore volume of water has been injected all oil could, in the ideal case, have been produced, but it is clear that because of the heterogeneous reservoir structure a lot of oil has been left behind; see the top-right figure. The second row of Fig. 7 depicts the results if the water flood is operated in 'closed-loop' using an ensemble of 100 coarse reservoir models of 100 grid blocks each with parameters that are frequently updated with EnKF during the flooding process. The figures at the bottom row show that the initial average permeability estimate is nearly uniform ($t = 0$ days), but that after a while a heterogeneous pattern has emerged ($t = 116$ days) that does not really change very much any more until the end of the flooding period ($t = 750$ days). As follows from comparison of the final (rightmost) figures in the first two rows, the optimized water flooding strategy results in a significantly improved oil recovery. In this example the initial ensembles did not show a marked heterogeneity, but just a Gaussian random spatial structure, and therefore we based the optimization on the ensemble average, rather than using a robust strategy as in the previous example. The third row in Fig. 7 shows the flow rates in the 10 injection wells and illustrates that the optimization results in a dynamic strategy of closing and opening different valves over time.

7. DISCUSSION

The concept of closed-loop reservoir management and production optimization has been described in different forms before; see e.g. Chierici (1992), or Nyhavn (2000), with further references given in Jansen et al. (2005). However none of these papers makes use of systematic techniques for both optimization and data assimilation. The examples shown in this paper are simplistic, and in a realistic field, with realistic well constraints, the scope for optimization will be smaller.
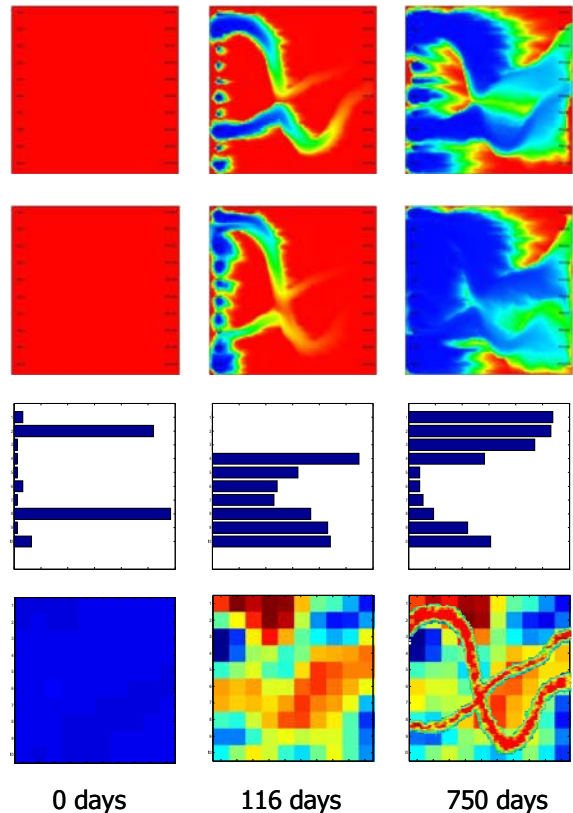

0 days   116 days   750 days

Fig. 7. Snapshots in time. Top row: saturations during conventional water flooding (red: oil, blue: water). Second row: Saturations during closed-loop optimized water flooding. Third row: Flow rates in the injection wells. Bottom row: estimated permeability field (average of 100 ensemble members). Note: The bottom-right figure has been overlain with the 'true' channel structure from Fig. 6. (After Overbeek et al. (2004)).

However, the examples illustrate some essential aspects of our closed-loop management approach:

- Systematic optimization of well rates over the producing life of a reservoir produced with water flooding offers scope for increased oil recovery and reduced water production.
- The effect of uncertain reservoir parameters can be reduced through a) robust optimization over an ensemble of reservoir models, and b) regular updating of the models using production data.
- A relatively simple reservoir model may still give acceptable results when used for optimization of a fixed configuration of injection and production wells.

Especially the last point raises some interesting system-theoretical questions which are topic of our current research. The observability of reservoir pressures (which are required to estimate the permeabilities) from the wells is probably very small because of the diffuse nature of pressure propagation in porous media. However the controllability of the pressure field (which drives the saturation changes) is equally limited, which explains why a relatively simple model works so well to optimize flooding in a fixed configuration of wells. We note that this would to a much lesser extent be true if we were to drill new wells, in which case additional geological

information would be required. Another, more practical, aspect of our research that requires input from measurement and control theory involves the combination of short-term production optimization and long-term reservoir management. This will probably require a layered control structure, as commonly used in the process industry where longer term optimization results serve as constraints for the short-term optimization, which in turn provides set points for field controllers; see e.g. Saputelli et al (2006). In conclusion, there appears to be ample scope to use a variety of results from process control theory and practice, in particular for optimization, parameter estimation and model reduction, to further develop the techniques for model-based control of subsurface flow

REFERENCES

Asheim, H. (1988). Maximization of water sweep efficiency by controlling production and injection rates. Paper SPE 18365 presented at the SPE European Petroleum Conference, London, UK, October 16-18.

Aziz, K. and Settari, A. (1979). *Petroleum reservoir simulation*. Applied Science Publishers, London.

Bennett, A.F. (2002). *Inverse modeling of the ocean and atmosphere*, Cambridge University Press, Cambridge.

Brouwer, D.R. and Jansen, J.D. (2004). Dynamic optimization of water flooding with smart wells using optimal control theory. *SPE Journal*, December, 391-402.

Brouwer, D.R., Nævdal, G., Jansen, J.D., Vefring, E.H. and van Kruijsdijk, C.P.J.W. (2004). Improved reservoir management through optimal control and continuous model updating. Paper SPE 90149 presented at the SPE Annual Technical Conference and Exhibition, Houston, Texas, USA, 26-29 September.

Caers, J. (2003). History matching under training-image-based geological model constraints. *SPE Journal*, September, 218-226.

Chavent, G., Dupuy, M. and Lemonnier, P. (1975). History matching by use of optimal theory. *SPE Journal*, February, 74-86.

Chierici, G.L. (1992). Economically improving oil recovery by advanced reservoir management. *Journal of Petroleum Science and Engineering* **8**, 205-219.

Erbaş, D. and Christie, M.A. (2007). Effect of sampling strategies on prediction uncertainty estimation. Paper SPE 106229, presented at the SPE Reservoir Simulation Symposium, Houston, USA, 26-28 February.

Esmaiel, T.E.H., Fallah, S. and Van Kruijsdijk, C.P.J.W. (2005). Determination of WAG ratios and slug sizes under uncertainty in a smart wells environment. Paper SPE 93569 presented at the 14th SPE Middle East Oil and Gas Show and Conference, Bahrain, 12-15 March.

Evensen, G. (2006). *Data assimilation*. Springer, Berlin.

Ewing, R.E. (1983). Problems arising in the modeling of processes for hydrocarbon recovery. In: *The mathematics of reservoir simulation* (Ewing, R.E. (ed.)). SIAM, Philadelphia.

Gildin, E., Klie, H., Rodriguez, A., Wheeler, M.F. and Bishop, R.H. (2006). Development of low-order controllers for high-order reservoir models and smart wells. Paper SPE 102214 presented at the SPE Annual Technical Conference and Exhibition, San Antonio, USA, 24-27 September.

Gill, P.E., Murray, W. and Wright, M.H. (1981). *Practical optimization*. Academic Press, London.

Güyagüler, B. and Horne, R. (2004). Uncertainty assessment of well-placement optimization. *SPE Reservoir Evaluation and Engineering*, February, 24-32.

Handels, M., Zandvliet, M.J., Brouwer, D.R. and Jansen, J.D. (2007). Adjoint-based well placement optimization under production constraints. Paper SPE 105797 presented at the SPE Reservoir Simulation Symposium, Houston, USA, 26-28 February.

Heijn, T., Markovinović, R. and Jansen, J.D. (2004). Generation of low-order reservoir models using system-theoretical concepts'. *SPE Journal*, June, 202-218.

Jafarpour, B. and McLaughlin, D. (2007). Efficient permeability parameterization with the discrete cosine transform. Paper SPE 106453 presented at the SPE Reservoir Simulation Symposium, Houston, USA, 26-28 February.

Jansen, J.D., Brouwer, D.R., Nævdal, G. and van Kruijsdijk, C.P.J.W. (2005). Closed-loop reservoir management. *First Break*, **23**, 43-48.

Kraaijevanger, J.F.B.M., Egberts, P.J.P., Valstar, J.R. and Buurman, H.W. (2007). Optimal waterflood design using the adjoint method. Paper SPE 105764 presented at the SPE Reservoir Simulation Symposium, Houston, USA, 26-28 February.

Li, R., Reynolds, A.C., and Oliver, D.S. (2003). History matching of three-phase flow production data. *SPE Journal*, December, 328-340.

Lien, M., Brouwer, D.R., Manseth, T. and Jansen, J.D. (2006). Multiscale regularization of flooding optimization for smart field management. Paper SPE 99728 presented at the SPE Intelligent Energy Conference and Exhibition, Amsterdam, The Netherlands, April 11-13.

Markovinović, R. and Jansen, J.D. (2006). Accelerating iterative solution methods using reduced-order models as solution predictors, *International Journal of Numerical Methods in Engineering*, **68**, 525-541.

Montleau, P., Cominelli, A., Neylon, K. and Rowan, D. (2006). Production optimization under constraints using adjoint gradients. *Proc. 10th European Conference on the Mathematics of Oil Recovery (ECMOR X)*, Amsterdam, The Netherlands, September 4-7.

Nævdal, G., Johnsen, L.M., Aanonsen, S.I. and Vefring, E.H. (2005). Reservoir monitoring and continuous model updating using ensemble Kalman filter. *SPE Journal*, January, 66-74.

Nævdal, G., Brouwer, D.R., and Jansen, J.D. (2006). Waterflooding using closed-loop control. *Computational Geosciences*, **10**, No.1, 37-60.

Naus, M.M.J.J., Dolle, N. and Jansen, J.D. (2006). Optimisation of commingled production using infinitely variable inflow control valves. *SPE Production and Operations*, May, 293-301.

Nyhavn, F., Vassenden, F. and Singstad, P. (2000). Reservoir drainage with down hole permanent monitoring and control systems. Paper SPE 62937 presented at the SPE Annual Technical Conference and Exhibition, Dallas, Texas, USA, 1-4 October.

Overbeek, K.M., Brouwer, D.R., Nævdal, G. and van Kruijsdijk, C.P.J.W. (2004). Closed-loop waterflooding. *Proc.* 9th European Conference on the Mathematics of Oil Recovery (ECMOR IX), Cannes, France, August 28 – September 2.

Peaceman, D.W. (1977). *Fundamentals of numerical reservoir simulation*. Elsevier, Amsterdam.

Przybysz-Jarnut, J.K., Hanea, R.G., Jansen, J.D. and Heemink, A.W. (2007). Application of the representer method for parameter estimation in numerical reservoir models. *Computational Geosciences,* **11**, No. 1, 73-85.

Ramirez, W.F. (1987). *Application of optimal control theory to enhanced oil recovery.* Elsevier, Amsterdam.

Rommelse, J.R., Kleptsova, O., Jansen, J.D. and Heemink, A.W. (2006). Data assimilation in reservoir management using the representer method and the ensemble Kalman filter. *Proc.* 10th European Conference on the Mathematics of Oil Recovery (ECMOR X), Amsterdam, Netherlands, September 4-7.

Saputelli, L., Nikolaou, M. and Economides, M.J. (2006). Real-time reservoir management: A multiscale adaptive optimization and control approach. *Computational Geosciences*, **10**, No. 1, 61-96.

Sarma, P., Aziz, K. and Durlofsky, L.J. (2005). Implementation of adjoint solution for optimal control of smart wells. Paper SPE 92864 presented at the SPE Reservoir Simulation Symposium, Houston, USA, 31 January – 2 February.

Sarma, P., Chen, W.H. (2006a). Production optimization with adjoint models under nonlinear control-state path inequality constraints. Paper SPE 99959 presented at the SPE Intelligent Energy Conference and Exhibition, Amsterdam, The Netherlands, April 11-13.

Sarma, P., Durlofsky, L.J., Aziz, K. and Chen, W.H., (2006b). Efficient real-time reservoir management using adjoint-based optimal control and model updating. *Computational Geosciences,* **10**, No. 1, 3-36.

Smil, V. (2003). *Energy at the crossroads.* MIT Press, Cambridge.

Stengel, R.F. (1994). *Optimal control and estimation.* Dover, New York.

Sudaryanto, B., and Yortsos, Y.C. (2000). Optimization of fluid front dynamics in porous media using rate control. *Physics of Fluids* **12**, No.7, 1656-1670.

Van Doren, J.F.M., Markovinović, R. and Jansen, J.D. (2006). Reduced-order optimal control of waterflooding using POD. *Computational Geosciences*, **10**, 137-158, DOI: 10.1007/ s10596-005-9014-2.

Van Essen, G.M., Zandvliet, M.J., Van den Hof, P.M.J., Bosgra, O.H. and Jansen, J.D. (2006). Robust optimization of oil reservoir flooding. Paper WeB10.3 presented at the IEEE joint CCA, ISIC and CACSD, Munich, Germany, October 4-6.

Vasco, D.W., Soon, S. and Datta-Gupta, A (1999). Integrating dynamic data into high-resolution reservoir models using streamline-based analytical sensitivity coefficients. *SPE Journal*, 389-399.

Virnovski, G.A. (1991). Waterflooding strategy design using optimal control theory", *Proc.* 6th European Symp. on IOR, Stavanger, Norway, 437-446.

Yeten, B., Durlofsky, L.J. and Aziz, K. (2003). Optimization of nonconventional well type, location and trajectory. *SPE Journal*, September, 200-210.

Zakirov, I.S., Aanonsen, S.I., Zakirov, E.S., and Palatnik, B.M. (1996). Optimization of reservoir performance by automatic allocation of well rates," *Proc.* 5th European Conference on the Mathematics of Oil Recovery (ECMOR V), Leoben, Austria.

Zandvliet, M.J., Bosgra, O.H., Jansen, J.D., Van den Hof, P.M.J. and Kraaijevanger, J.F.B.M. (2007). Bang-bang control and singular arcs in reservoir flooding. *Journal of Petroleum Science and Engineering*. In press. Published online. DOI:10.1016/ j.petrol.2006.12.008

ACKNOWLEDGEMENTS

APPENDIX A: NUMERICAL SIMULATION OF SUBSURFACE FLOW

As in all branches of fluid mechanics, the physics of flow through a porous medium can be described with the aid of partial differential equations that represent conservation of mass, momentum and energy, and equations of state that describe the fluid properties as a function of pressure and temperature. Except in case of steam flooding we can assume that reservoir

flow is isothermal, which implies that we may disregard the energy balance equation. Moreover, the movement of fluids is usually so slow that we can disregard inertial effects, and that instead of the momentum balance equation we may use an empirical relationship between pressure drop and flow velocity known as Darcy's law. For the simple case of two-phase (oil-water) flow we can write the mass balance equation for each phase in vector notation as

$$\nabla \cdot (\rho_i \mathbf{v}_i) + \frac{\partial (\rho_i \phi S_i)}{\partial t} - \rho_i q_i''' = 0, \qquad (A.1)$$

where ρ is fluid density, $\mathbf{v}$ is (superficial) fluid velocity, ϕ is porosity, S is fluid saturation of the pore space ($0 \le S \le 1$), t is time, q''' is flow rate per unit volume, and the subscript $i \in \{o, w\}$ indicates the oil and water phases respectively. Darcy's law can be expressed as

$$\mathbf{v}_i = -\frac{k_{ri}}{\mu_i} \mathbf{K} (\nabla p_i - \rho_i g \nabla d), \qquad (A.2)$$

where $\mathbf{K}$ is the permeability tensor, μ fluid viscosity, k_r relative permeability, p pressure, g acceleration of gravity and d depth. The permeability tensor $\mathbf{K}$, whose elements have units of surface area, represents how easily the fluids flow through the rock in different directions. Usually the orientation of the coordinate system can be aligned with the geological layering in the reservoir such that $\mathbf{K}$ is a diagonal matrix:

$$\mathbf{K} = diag(k_x, k_y, k_z), \qquad (A.3)$$

where k_x, k_y and k_z are directional permeabilities in the x, y and z coordinate directions. The dimensionless relative permeabilities k_{ri} are functions of S, and are reduction factors that represent the increase in flow resistance caused by multi-phase effects. The resistance to concurrent flow of oil and water is generally much higher than the sum of the resistances to flow of the individual phases, and the relative permeabilities are therefore a major source of nonlinearity in the multi-phase equations. Combining equations (A.1) and (A.2) results in

$$-\nabla \cdot \left[\frac{\rho_i k_{ri}}{\mu_i} \mathbf{K} (\nabla p_i - \rho_i g \nabla d) \right] + \frac{\partial (\rho_i S_i \phi)}{\partial t} - \rho_i q_i''' = 0. \qquad (A.4)$$

Equation (A.4) contains four unknowns, p_w, p_o S_w and S_o, two of which can be eliminated with aid of the relationships

$$S_w + S_o = 1, \qquad (A.5)$$

$$p_o - p_w = p_c(S_w), \qquad (A.6)$$

where $p_c(S_w)$ is the oil-water capillary pressure which is another source of nonlinearity in the flow equations. Substituting equations (A.5) and (A.6) in equations (A.4), expanding the right-hand sides, applying chain-rule differentiation, substituting the isothermal equations of state, expressed as oil and water compressibilities

$$c_o = \frac{1}{\rho_o} \frac{\partial \rho_o}{\partial p_o} \bigg|_{T_R}, \qquad (A.7)$$

$$c_w = \frac{1}{\rho_w} \frac{\partial \rho_w}{\partial p_w} \bigg|_{T_R} \approx \frac{1}{\rho_w} \frac{\partial \rho_w}{\partial p_o} \bigg|_{T_R},$$

and substituting the rock compressibility

$$c_r = \frac{1}{\phi} \frac{\partial \phi}{\partial p_o}, \qquad (A.8)$$

allows us to express equations (A.4) in terms of p_o and S_w as follows:

$$-\nabla \cdot \left\{ \frac{\rho_w k_{rw}}{\mu_w} \mathbf{K} \left[\left(\nabla p_o - \frac{\partial p_c}{\partial S_w} \nabla S_w \right) - \rho_w g \nabla d \right] \right\} + \\ \rho_w \phi \left[S_w (c_w + c_r) \frac{\partial p_o}{\partial t} + \frac{\partial S_w}{\partial t} \right] - \rho_w q_w''' = 0, \qquad (A.9)$$

$$-\nabla \cdot \left[\frac{\rho_o k_{ro}}{\mu_o} \mathbf{K} (\nabla p_o - \rho_o g \nabla d) \right] + \\ \rho_o \phi \left[(1 - S_w)(c_o + c_r) \frac{\partial p_o}{\partial t} - \frac{\partial S_w}{\partial t} \right] - \rho_o q_o''' = 0. \qquad (A.10)$$

The two-phase flow equations as formulated in expressions (A.9) and (A.10) contain two state variables: the oil pressure p_o and the water saturation S_w. The equations are nonlinear because of the saturation dependence of the capillary pressure p_c and the relative permeabilities k_r. In the more general case there may also be a pressure dependency of the densities ρ, the porosity ϕ, and the compressibilities c, in particular if the formulation is extended to include gas as a third phase. The nature of the equations is discussed in e.g. Peaceman (1977), Aziz and Settari (1979) and Ewing (1983). It can be shown that the pressure behavior is essentially diffusive, i.e. that the corresponding equations are parabolic and become elliptic in the limit of zero compressibility. The saturation behavior is mixed diffusive-convective, i.e. the corresponding equations are mixed parabolic-hyperbolic and become completely hyperbolic in the case of zero capillary pressure. The equations can be discretized in space and time. Most numerical reservoir simulators apply a spatial discretization scheme based on finite difference or finite volume formulations, using an upstream weighting in the convection-dominated terms. In a simplified case where we disregard the effects of capillary pressure, and gravity, and where we assume that the input consists of prescribed flow rates in the wells only, we obtain a system of nonlinear first-order differential equations that can be expressed as

$$\begin{bmatrix} \mathbf{V}_{wp}(\mathbf{s}) & \mathbf{V}_{ws} \\ \mathbf{V}_{op}(\mathbf{s}) & \mathbf{V}_{os} \end{bmatrix} \begin{bmatrix} \dot{\mathbf{p}} \\ \dot{\mathbf{s}} \end{bmatrix} + \begin{bmatrix} \mathbf{T}_w(\mathbf{s}) & \mathbf{0} \\ \mathbf{T}_o(\mathbf{s}) & \mathbf{0} \end{bmatrix} \begin{bmatrix} \mathbf{p} \\ \mathbf{s} \end{bmatrix} = \begin{bmatrix} \mathbf{q}_w \\ \mathbf{q}_o \end{bmatrix}, (A.11)$$

where $\mathbf{p}$ and $\mathbf{s}$ are vectors of pressures p_o and water saturations S_w respectively, $\mathbf{V}$ is an accumulation matrix (containing the parameters ϕ, c_o, c_w and c_r), $\mathbf{T}$ is a transmissibility matrix (containing the parameters k, k_r and μ), and $\mathbf{q}_o$ and $\mathbf{q}_w$ are vectors of oil and water flow rates with non-zero elements corresponding to gridblocks penetrated by a well. Both $\mathbf{V}$ and $\mathbf{T}$ are functions of $\mathbf{s}$, either directly or

through the parameters. In injection wells we can prescribe $\mathbf{q}_w$, while $\mathbf{q}_o$ is equal to zero. In production wells we can not directly control $\mathbf{q}_o$ and $\mathbf{q}_w$, but we can control the total flow rates $\mathbf{q}_t = \mathbf{q}_o + \mathbf{q}_w$ as

$$\begin{bmatrix} \mathbf{q}_w \\ \mathbf{q}_o \end{bmatrix} = \begin{bmatrix} \mathbf{F}_w(\mathbf{s}) \\ \mathbf{F}_o(\mathbf{s}) \end{bmatrix} \mathbf{q}_t, \qquad (A.12)$$

where $\mathbf{F}_w$ and $\mathbf{F}_o$ are diagonal matrices with saturation-dependent terms which add more nonlinearities to the system. Further complexities occur when we prescribe pressures in the wells rather than flow rates, ands when we take in to account the effects of capillary pressures and gravity. Moreover, reservoir simulators usually also model a third phase, gas, which has a pressure-dependent oil-solubility. A next step in complexity is obtained when individual hydrocarbon components are modeled, rather than just oil and gas, or when chemical interactions or thermal effects are taken into account; see e.g. Aziz and Settari (1979). However in all these cases it is possible to obtain a set of system equations which can be expressed in a form similar to equation (A.11), or more compactly, as

$$\mathbf{V}(\mathbf{x})\dot{\mathbf{x}} + \mathbf{T}(\mathbf{x})\mathbf{x} = \mathbf{F}(\mathbf{x})\mathbf{q}, \qquad (A.13)$$

where $\mathbf{x} = [\mathbf{p}, \mathbf{s}]^T$. Equation (A.13) can be recasted in a generalized nonlinear state space form

$$\mathbf{f}_1(\mathbf{x}, \boldsymbol{\theta}_1)\dot{\mathbf{x}} = \mathbf{f}_2(\mathbf{x}, \mathbf{u}, \boldsymbol{\theta}_2), \qquad (A.14)$$

where we have introduced the parameter vectors $\boldsymbol{\theta}_1$ and $\boldsymbol{\theta}_2$. The input vector $\mathbf{u}$ is related to the vector of well flow rates $\mathbf{q}$ as $\mathbf{u} = \mathbf{L}_{uq}\mathbf{q}$, with a selection matrix $\mathbf{L}_{uq}$ that selects the non-zero elements of $\mathbf{q}$, i.e. those elements that correspond to grid blocks penetrated by a well. For a reservoir model with n grid blocks and m wells, and modeling two phases only, we therefore have a state vector $\mathbf{x}$ and an input vector $\mathbf{u}$ of dimensions $2n$ and m respectively. The parameter vectors were introduced to represent those parameters that are uncertain and that need to be identified or updated during the reservoir management process. In the examples in this paper we restricted the parameter uncertainty to a homogeneous permeability $k = k_x = k_y = k_z$, which however, may still be different in each grid block such that in our case $\boldsymbol{\theta}_1$ and $\boldsymbol{\theta}_2$ have dimensions 0 and n respectively. Time discretization of the space-discretized system equations is usually performed fully implicitly, which implies that each time step the nonlinear equations are solved iteratively using a Newton-Raphson scheme. Under the assumption that $\mathbf{f}_1$ is invertible, which is the case for most problems, we can rewrite equations (A.12) in classical nonlinear state space form as was done in equations (1) or (2) in the body of the text. We note that we only use this classical state space form to simplify the subsequent analysis. In an actual numerical implementation, the time discretization is always performed starting from the generalized form (A.12). Typical grid block sizes in a reservoir simulation model are in the order of tens to hundreds of meters in directions aligned with the geological layers, and meters to tens of meters in the direction perpendicular to the layers, and reservoir models may contain from tens of thousands up to a few

millions of grid blocks. Typical simulation time steps are in the order of weeks to months, and a single reservoir simulation of the producing life of a field requires hours to sometimes days of computing time.

APPENDIX B: ADJOINT-BASED OPTIMIZATION

Consider the optimization problem

$$\max_{\mathbf{u}_k} J, \quad k = 1, \ldots, K \qquad (B.1)$$

with objective function (6). We aim to compute the optimal control $\mathbf{u}_k$ with the aid of a gradient-based algorithm, which requires the derivatives of J with respect to $\mathbf{u}_k$. The problem in determining the derivatives is the indirect dependence of the variation δJ_{ik} in the objective function on a variation δu_{ik} of the input. Here, δu_{ik} means the variation of element i of vector $\mathbf{u}$ at time k. Each term J_k, at an arbitrary time $k = \kappa$, is not only a direct function of $\mathbf{u}_\kappa$, but also a function of $\mathbf{y}_\kappa$, which, through equation (5), is a function of $\mathbf{x}_\kappa$, which in turn, through equation (3), is a function of $\mathbf{u}_\kappa$. The variations should therefore be computed as

$$\delta J_{i\kappa} = \left(\frac{\partial J_\kappa}{\partial \mathbf{u}_\kappa} + \sum_{k=\kappa}^{K} \frac{\partial J_k}{\partial \mathbf{y}_k} \frac{\partial \mathbf{y}_k}{\partial \mathbf{x}_k} \frac{\partial \mathbf{x}_k}{\partial \mathbf{u}_\kappa} \right) \frac{\partial \mathbf{u}_\kappa}{\partial u_{i\kappa}} \delta u_{i\kappa}. \quad (B.2)$$

(Note the different subscripts k and κ). The term $\partial \mathbf{x}_k / \partial \mathbf{u}_\kappa$ gives problems because we need to solve the recursive system of discrete-time differential equations (3) to connect the state vectors $\mathbf{x}_k, k = \kappa + 1, \ldots, K$ to the input $\mathbf{u}_\kappa$. The complex dependence can be taken into account by considering equation (3) as a set of additional constraints to the optimization problem, and applying the technique of Lagrange multipliers to solve the constrained optimization problem. Moreover, we may formally also consider the initial condition (4) and the output equation (5) as constraints, and, setting aside the 'ordinary constraints' $\mathbf{c}$, we can therefore define a modified objective function

$$\bar{J} = \sum_{k=0}^{K-1} \left\{ \begin{array}{l} J_{k+1}(\mathbf{y}_{k+1}, \mathbf{u}_{k+1}) + \boldsymbol{\lambda}_0^T(\mathbf{x}_0 - \check{\mathbf{x}}) \\ + \boldsymbol{\lambda}_{k+1}^T \mathbf{g}_{k+1}(\mathbf{x}_k, \mathbf{x}_{k+1}, \mathbf{u}_{k+1}) \\ + \boldsymbol{\mu}_{k+1}^T[\mathbf{y}_{k+1} - \mathbf{h}_{k+1}(\mathbf{x}_{k+1})] \end{array} \right\}, \quad (B.3)$$

where the constraints have been 'adjoined' to J_k with the aid of vectors of Lagrange multipliers $\boldsymbol{\lambda}$ and $\boldsymbol{\mu}$. We can obtain a first-order description of the effect of changing $\mathbf{u}_k$ on the magnitude of $\bar{J}$, through taking the first variation of equation (B.3). A necessary condition for an optimum is stationarity of $\delta \bar{J}$ for all variations, which leads to the following set of equations:

$$\boldsymbol{\lambda}_1^T \frac{\partial \mathbf{g}_1}{\partial \mathbf{x}_0} + \boldsymbol{\lambda}_0^T = \mathbf{0}^T \qquad (B.4)$$

$$\boldsymbol{\lambda}_{k+1}^T \frac{\partial \mathbf{g}_{k+1}}{\partial \mathbf{x}_k} + \boldsymbol{\lambda}_k^T \frac{\partial \mathbf{g}_k}{\partial \mathbf{x}_k} - \boldsymbol{\mu}_k^T \frac{\partial \mathbf{h}_k}{\partial \mathbf{x}_k} = \mathbf{0}^T \qquad (B.5)$$

$$\boldsymbol{\lambda}_K^T \frac{\partial \mathbf{g}_K}{\partial \mathbf{x}_K} + \boldsymbol{\mu}_K^T \frac{\partial \mathbf{h}_K}{\partial \mathbf{x}_K} = \mathbf{0}^T \qquad (B.6)$$

$$\frac{\partial J_{k+1}}{\partial \mathbf{y}_{k+1}} + \boldsymbol{\mu}_{k+1}^T = \mathbf{0}^T \qquad (\text{B.7})$$

$$\frac{\partial J_{k+1}}{\partial \mathbf{u}_{k+1}} + \boldsymbol{\lambda}_{k+1}^T \frac{\partial \mathbf{g}_{k+1}}{\partial \mathbf{u}_{k+1}} = \mathbf{0}^T \qquad (\text{B.8})$$

$$\mathbf{g}^T\left(\mathbf{x}_k, \mathbf{x}_{k+1}, \mathbf{u}_{k+1}\right) = \mathbf{0}^T \qquad (\text{B.9})$$

$$\left(\mathbf{x}_0 - \breve{\mathbf{x}}\right)^T = \mathbf{0}^T \qquad (\text{B.10})$$

$$\left[\mathbf{y}_{k+1} - \mathbf{h}\left(\mathbf{x}_{k+1}\right)\right]^T = \mathbf{0}^T \qquad (\text{B.11})$$

The last three equations are identical to output equation (5), initial condition (4) and system equation (3), and are therefore automatically satisfied. Equation (B.8) represents the effect of changing the control on the value of the objective function, while keeping all other variables fixed. For a non-optimal control this term is not equal to zero, but then it is exactly the expression that we require to iteratively obtain the optimal control using a gradient-based algorithm. Equation (B.7) allows us to compute the Lagrange multipliers $\boldsymbol{\mu}_{k+1}$, $k = 0, \dots K\text{-}1$. Next we can use equation (B.6) to compute multiplier $\boldsymbol{\lambda}_K$ for the final discrete time K, and thereafter the discrete-time differential equation (B.5) to recursively compute the multipliers $\boldsymbol{\lambda}_k$ for times $k = 0, \dots K\text{-}1$. Finally, equation (B.4) represents the effect of changing the initial condition $\mathbf{x}_0$ on the value of the objective function, while keeping all other variables fixed. However, because we prescribed the initial condition through equation (4) this term is in our case only of theoretical relevance. Solution of the optimization problem now consists of repeating the following steps until the optimal control vector $\mathbf{u}_k$ has been found:

- 'Forward' simulation of the system equations (5), starting from initial conditions (4) and an initial choice for $\mathbf{u}_k$.
- 'Backward' simulation of the adjoint equations (B.5), starting from final conditions (B.6).
- Computation of the derivatives of J with respect to the controls $\mathbf{u}_k$ with the aid of equation (B.8).
- Computation of an improved estimate of $\mathbf{u}_k$, using the derivatives and a gradient-based optimization routine of choice.

Because of its computational efficiency in calculating the gradients of the objective function, adjoint-based optimization is particularly attractive for problems with a large number of control parameters.